AIP | The Journal of Chemical Physics

Transient cage formation around hot gold colloids dispersed in polymer solutions

F. Schwaiger, W. Zimmermann, and W. Köhler

Citation: J. Chem. Phys. **135**, 224905 (2011); doi: 10.1063/1.3665935
View online: http://dx.doi.org/10.1063/1.3665935
View Table of Contents: http://jcp.aip.org/resource/1/JCPSA6/v135/i22
Published by the American Institute of Physics.

Transient cage formation around hot gold colloids dispersed in polymer solutions

F. Schwaiger, W. Zimmermann, and W. Köhler[a)]
Physikalisches Institut, Universität Bayreuth, D-95440 Bayreuth, Germany

(Received 6 July 2011; accepted 15 November 2011; published online 13 December 2011)

Gold colloids dispersed in dilute to concentrated polymer solutions can efficiently be heated by laser irradiation and act as almost pointlike heat sources. In systems with positive Soret coefficients S_T of the polymer, such as solutions of polystyrene in toluene, the polymer can almost entirely be removed from the particle surface. The colloid attracts the solvent and a transient cage of low viscosity and dramatically enhanced mobility is formed, which follows the motion of the particle with a certain retardation. Based on a complete parameterization of $S_T(M, c, T)$, we analyze in detail the stationary temperature, concentration, and viscosity profiles. Depending on the polymer molar mass and concentration on the distance to the glass transition temperature, the negative or positive feedback-loops are established that lead to either attenuation or self-amplification of the polymer depletion. [doi:10.1063/1.3665935]

I. INTRODUCTION

Gold colloids are chemically and optically stable and their surface can be functionalized, e.g., biochemical or medical applications.[1] They can form fractal aggregates,[2] their agglomeration can be controlled by optical irradiation,[3] and they can be trapped by a focused laser beam.[3,4] The high absorption cross section of the plasmon resonance in combination with their optical stability makes gold colloids ideal candidates for almost pointlike heat sources. They can be used to insert significant amounts of energy by optical heating on length scales far below the diffraction limit,[5] and an increase of the effective particle diffusion coefficient of hot colloids in a simple solvent has recently been reported.[6]

In this work, we investigate laser-heated gold colloids dispersed in polymer solutions. In such multicomponent fluid mixtures there is a complex situation due to the coupling between temperature gradients and mass diffusion.[7] For small molecules this so-called Soret effect is quite subtle and the concentration change that can be induced by a temperature difference of 1 K is typically only one-tenth of a percent,[8] corresponding to Soret coefficients of $S_T \sim 10^{-3}$ K^{-1}. The situation can be quite different, however, in certain systems with slow dynamics and long correlation length. Comparatively, large Soret coefficients above 1 K^{-1} can be found for dilute solutions of high molar mass polymers[9] and colloidal dispersions.[10] Near a consolute critical point, the Soret coefficients exceed the ones normally measured for small molecules by more than four orders of magnitude.[11,12] Among other recently discovered phenomena[13,14] such a strong coupling of the concentration to the temperature field can be utilized, e.g., laser-patterning of near-critical and critical polymer blends.[15–17]

A colloidal gold particle embedded in a concentrated solution of polystyrene (PS) of arbitrary molar mass or in a semidilute solution of entangled long chains in toluene is almost immobile due to the very high viscosity of the matrix. When the gold particle is illuminated with a laser beam, the viscosity in the immediate neighborhood of the particle is dramatically reduced by orders of magnitude within fractions of a second. The solvent is attracted towards the hot surface and a localized pocket of high mobility dynamically forms around the colloid. If the colloid is displaced either by Brownian motion or by photonic forces exerted by the laser beam, the matrix adjusts to the new position and the pocket of high mobility follows the particle with a certain retardation. In particular, during rapid displacement over micrometer distances, as can be observed by anti-tweezing effects near the boundary of a laser focus, the mobility bubble cannot follow the particle motion fast enough and the colloidal motion comes to a rest at the almost rigid walls of this transient cage.

In the following, we will investigate the mechanisms that lead to the cage or bubble formation. We will focus, in particular, on the stationary state of the temperature and concentration fields around a colloid, which is rapidly established. Depending on the particular choice of the system, the viscosity in the immediate vicinity of the colloid can change by many orders of magnitude either due to a reduction of entanglement effects or due to an increasing distance to the glass transition. We will show that the first mechanism is more effective, since it is related to an increase of the correlation length of the polymer solution, which in turn leads to a positive feedback loop.

II. MODEL

The scenario leading to the mobility bubble is much more complex and efficient than a simple viscosity reduction caused by the local temperature increase. The main mechanism is due to a polymer depletion and, consequently, solvent enrichment around the heated colloid caused by the Soret effect.

a)Author to whom correspondence should be addressed. Electronic mail: werner.koehler@uni-bayreuth.de.

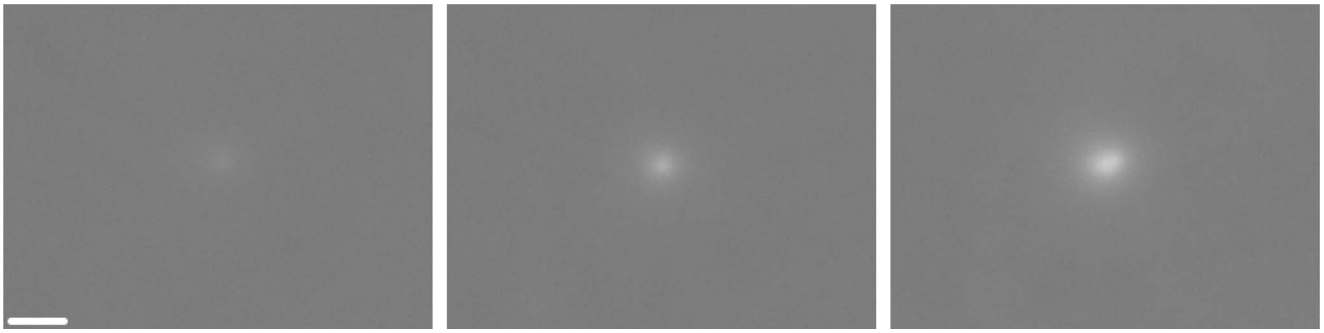

FIG. 1. Phase contrast images of temperature and concentration bubble around a laser-heated gold colloid in PS/toluene ($M = 17.7$ kg/mol, $c = 0.5$). The surface temperature increases are $T(R) = 4$ K (left), $T(R) = 13$ K (middle), and $T(R) = 30$ K (right). The laser beam has been mildly focused to a diameter of 26 μm (width at e^{-2}). For a better visibility, the image with zero laser intensity has been subtracted from all images. Scale bar 5 μm.

A decrease of the polymer concentration leads to a decrease of the viscosity for two quite different reasons. First, the topological chain entanglements, which are responsible for the high viscosity of polymer melts even at elevated temperatures, become less important. This effect is usually described within the framework of the reptation model[18] and strongly depends on the chain length of the polymer. Second, a polymer solution can be regarded as a binary glass former composed of two components with a high T_g-contrast, where the solvent acts as a plasticizer for the polymer. A solvent enrichment lowers the glass transition temperature and, thus, increases the distance to the glass transition. This effect does not depend on the molar mass for chains exceeding ~100 repeat units.[19] The distance to the glass transition determines the local friction experienced by the polymer segments.

Since the radius of our colloids exceeds the longest length scale present in the polymer solution, the radius of gyration of a polymer coil, they experience the macroscopic shear viscosity that incorporates both local friction effective on a molecular (solvent) length scale and the polymer entanglements. Before we come to a more detailed discussion of these two friction mechanisms, we first have to discuss how the concentration profile around the colloid is established.

As a motivating example, Fig. 1 shows the phase contrast images of a single laser-heated gold colloid of $R = 125$ nm radius in a solution of PS/toluene. Since the phase contrast technique visualizes the change of the refractive index, the visible bubble contains contributions from both the temperature rise and the polymer depletion around the colloid. A detailed analysis, based on the ideas that will be developed in the following, shows that the polymer concentration change causes the major contribution (~75%) to the signal in Fig. 1, but the effect of the temperature on the refractive index change is, albeit smaller, not negligible.

A. The stationary state

A detailed analysis of the coupled time-dependent heat equation and the time-dependent diffusion equations for the polymer and the colloid requires considerable effort. Significant insight into the effect can, however, already be gained from the stationary concentration and viscosity profiles around an isolated colloid embedded within an infinite medium.

After the laser is turned on, the stationary temperature profile

$$T(r) = \frac{\dot{Q}}{4\pi\kappa r} + T_0 = (T(R) - T_0)\frac{R}{r} + T_0 \tag{1}$$

is established almost instantaneously.[20] $T(R) = \dot{Q}/(4\pi\kappa R) + T_0$ is the temperature at the surface of the colloid of radius R, T_0 is the bulk temperature, κ is the thermal conductivity of the polymer solution, and $\dot{Q}$ is the optical power absorbed by the particle. The optical properties of gold nanospheres can be calculated from the Mie theory. For objects of the size of 100 nm both the scattering and the absorption cross section are of comparable magnitude and can be estimated by the geometrical cross section of the colloid, if the excitation occurs in the plasmon absorption band.[21] An estimation of the temperature increase of a colloid ($R \sim 0.1$ μm) in a polymer solution ($\kappa \sim 0.1$ W /(m K)) illuminated with an unfocused laser beam (1 W/mm^2) yields $T(R) - T_0 \sim 0.25$ K. Mild focusing to a beam waist of 50 μm is sufficient for a temperature rise of 100 K. Because of the radial symmetry and the rapid decay of $T(r)$, heated colloids allow for a much stronger localization of the temperature field than would be possible by bulk absorption of even a sharply focused laser beam.

As a consequence of the temperature gradient, a thermodiffusive flux

$$\vec{j}_T = -\rho D_T c(1-c)\nabla T \tag{2}$$

of the polymer with respect to the solvent sets in Ref. 7. c is the polymer mass fraction, ρ is the density of the solution, and D_T is the thermal diffusion coefficient. For the system PS/toluene, D_T is always positive and the direction of $\vec{j}_T$ such that PS is transported down the temperature gradient, away from the colloid. Toluene, on the other hand, is enriched near the hot particle surface.

The build-up of the concentration gradient, in turn, causes a Fickian diffusion current $\vec{j}_c = -\rho D\nabla c$ that tends to re-establish a homogeneous polymer concentration. In the stationary state, the total diffusion current vanishes

$$\vec{j} = \vec{j}_c + \vec{j}_T = -\rho D\nabla c - \rho D_T c(1-c)\nabla T = 0. \tag{3}$$

B. The Soret coefficient

In order to continue we need information about the temperature and concentration dependence of the Soret coefficient $S_T = D_T/D$. To our knowledge, PS/toluene is the only polymer solution where the entire molar mass and concentration dependence of S_T has ever been determined, at least at room temperature.[9]

From the experimental data published in Refs. 9 and 22, which cover a molar mass range from 4.75 kg/mol to 4060 kg/mol, and from a series of own temperature-dependent measurements, an empirical parameterization of $S_T(M, c, T)$ can be found

$$S_T(M, c, T) = S_T(M, c, T_0)\left(\frac{T_0}{T}\right)^{\gamma}, \tag{4}$$

$$S_T(M, c, T_0) = \frac{a}{1 + b\,c^{\beta}}, \tag{5}$$

$$a = 3.294 \times 10^{-4}\, M^{0.58}, \tag{6}$$

$$\beta = 35.42\, M^{-0.5} + 0.82, \tag{7}$$

$$b = \frac{a}{0.012} - 1, \tag{8}$$

$$\gamma = 2.4. \tag{9}$$

The reference temperature is $T_0 = 298$ K. M is the molar mass in g/mol. All concentration and molar mass dependence is contained in $S_T(M, c, T_0)$.

Above parameterization not only provides a good description of the data but is also physically well motivated for certain limiting cases. In the dilute limit, the scaling relation of the hydrodynamic radius is reflected in $S_T(M, c = 0, T_0) = 3.294 \times 10^{-4}\, M^{0.58}$, with an exponent very close to the Flory exponent $\nu = 0.588$. This scaling law for S_T can be rationalized by the constant molar mass independent thermal diffusion coefficient $D_T(c \to 0)$ (Refs. 23 and 24) in combination with the scaling law of the diffusion coefficient $D(c \to 0) \sim M^{-\nu}$. For overlapping chains, in the semidilute and concentrated regimes, the molar mass dependence vanishes very similar to the corresponding behaviour of the collective diffusion coefficient.[9,25] A common value of $S_T(M, c = 1, T_0) = 0.012\ \mathrm{K}^{-1}$ is assumed, and also the slope $(dS_T/dc)(M, c = 1, T_0) \approx -0.01\ \mathrm{K}^{-1}$ is essentially independent of M. It is worth mentioning that the glass transition, which severely slows down both mass and thermal diffusion, has no influence on the Soret coefficient S_T.[9]

The experimental data are shown together with the parameterization in Fig. 2. For the highest molar mass data ($M = 4060$ kg/mol), the Soret coefficient changes by almost 2.5 orders of magnitude from the concentrated to the dilute limit. Although there is a slight systematic under-estimation of S_T for high molar masses and concentrations around $c = 0.3$, Eq. (4) provides an almost perfect and not unnecessarily complicated analytical parameterization for the purpose of the following discussions.

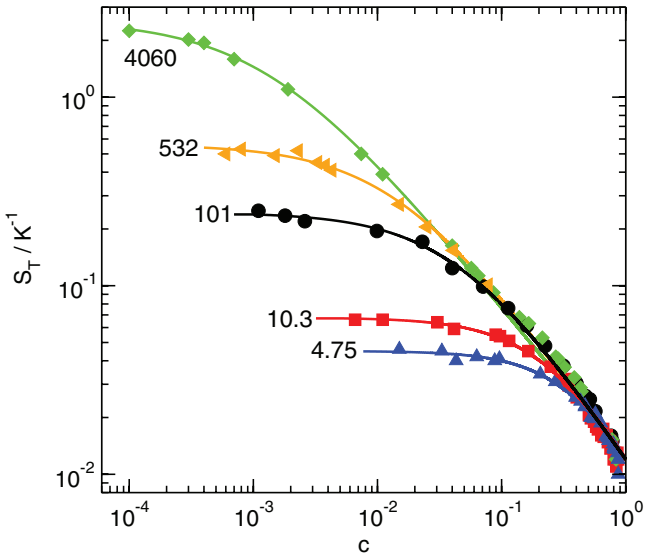

FIG. 2. Parameterization of the Soret coefficient S_T of PS/toluene at $T_0 = 298$ K as a function of PS concentration (mass fraction) c and molar mass M (kg/mol) according to Eq. (5). Experimental data from Ref. 9. The solid lines correspond to the fit of Eq. (4).

An alternative unifying scaling relation with a master plot for S_T of semidilute PS/toluene solutions has been proposed by Zhang *et al.*[26] The agreement with the experimental data from our laboratory (Fig. 2) is, however, not satisfactory, with deviations by a factor of two for the highest molar mass in the dilute limit. Furthermore, such a scaling relation for the dilute regime cannot be expected to hold up to the concentrated limit.

Since no literature data for the temperature dependence of S_T existed, we have performed own measurements for a series of PS weight fractions between 0.01 and 0.76 for a representative molar mass of $M = 90$ kg/mol (see Fig. 3) by means of the transient holographic grating technique of

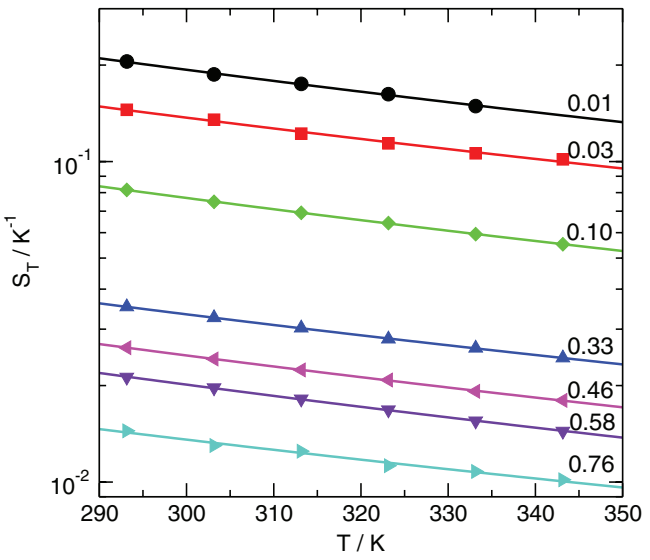

FIG. 3. Temperature dependence of the Soret coefficient for different PS ($M = 90$ kg/ mol) concentrations (mass fractions) between $c = 0.01$ and $c = 0.76$. The solid lines are fits with $S_T \propto T^{-\gamma}$ with $\gamma = 2.4 \pm 0.1$.

thermal diffusion forced Rayleigh scattering (TDFRS).[27] Within the errors all concentrations are well described by a power law $S_T \propto T^{-\gamma}$ with $\gamma = 2.4 \pm 0.1$ as used in Eq. (9). Since S_T is molar mass independent above the overlap concentration and since the identical exponent is found both for the dilute and semidilute solutions, it appears reasonable to assume the same temperature dependence also for all other PS molar masses and concentrations.

C. The concentration profile

Knowing $T(r)$ and $S_T(M, c, T)$ the stationary concentration profile $c(r)$ can be calculated. If the colloid is sufficiently far away from a wall, the problem has spherical symmetry, and from Eqs. (1), (3), and (4) we obtain after separation of the variables c and r for the stationary state

$$\frac{1 + b\,c^{\beta}}{a\,c(1-c)}\,dc = \left(\vartheta\frac{R}{r} + 1\right)^{-\gamma} T_0\,\vartheta\frac{R}{r^2}\,dr\,. \tag{10}$$

Here, we have additionally defined the dimensionless temperature rise

$$\vartheta = \frac{T(R) - T_0}{T_0}\,. \tag{11}$$

The molar mass dependence is introduced via a, b, and β according to Eqs. (4)–(8).

Far away from the colloid the polymer concentration retains its initial value $c = c_0$. The concentration $c(r)$ at a distance $r \geq R$ from the center of the particle is obtained after numerically integrating the left side of Eq. (10) from $c(r)$ to c_0 and the right side from r to infinity and solving for $c(r)$.

Figs. 4 and 5 show, as examples, the stationary distribution of the polymer ($M = 100$ kg/mol) up to 2 μm distance from the colloid for two different initial polymer concentrations of $c_0 = 0.5$ and $c_0 = 0.1$, respectively. The concentration is plotted over the (x, y)-plane. The third spatial coordinate

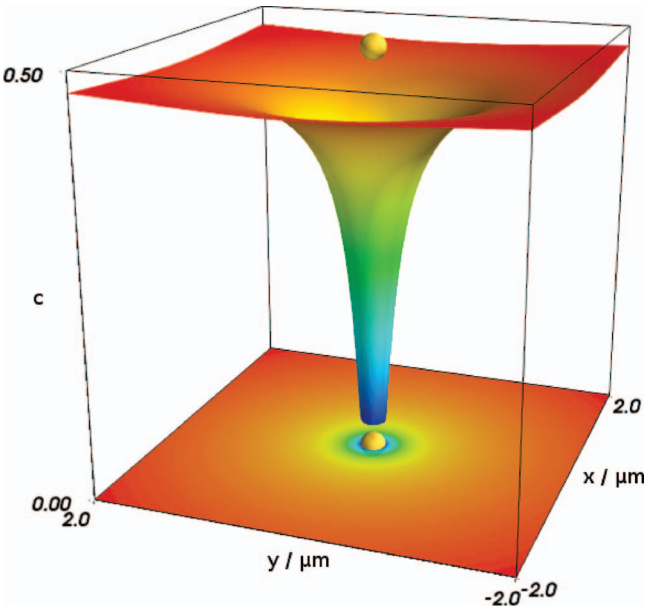

FIG. 4. Stationary localized concentration (mass fraction) bubble around a heated gold colloid. $M = 100$ kg/mol, $T(R) = 395$ K, and $c_0 = 0.5$.

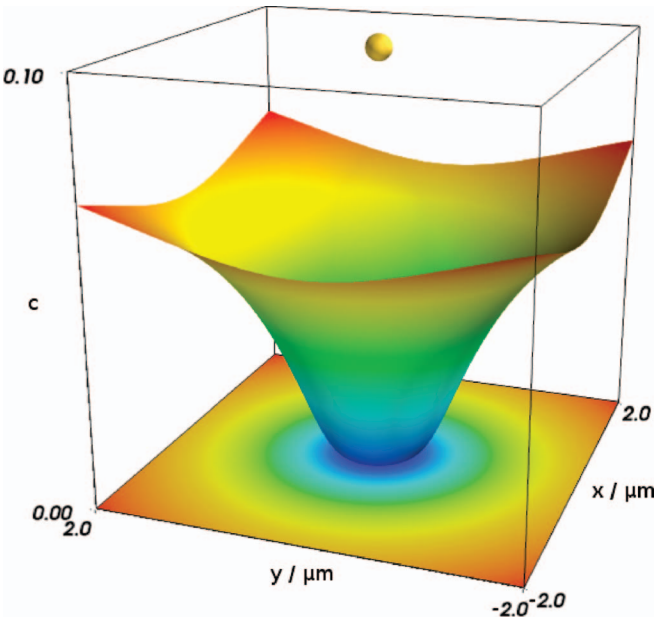

FIG. 5. Stationary localized concentration (mass fraction) bubble around a heated gold colloid. $M = 100$ kg/mol, $T(R) = 395$ K, and $c_0 = 0.1$.

(z) has been sacrificed. The surface temperature $T(R)$ is always 100 K above room temperature, which is easily achievable in a focused laser beam. The Au-colloid ($R = 125$ nm) is on scale. In the case of $c_0 = 0.5$ (Fig. 4), the polymer is almost completely repelled from the colloid ($c \approx 0.03$ at the surface). The localization of the concentration bubble is still strong with a diameter of only 0.5 μm (fwhm). With an initial concentration of $c_0 = 0.1$ (Fig. 5), the diameter of the solvent-rich pocket increases to $\sim$3 μm, and practically no polymer is left in the immediate vicinity of the colloid ($c < 10^{-5}$). Fig. 6 shows $c(r)$ for the same system ($M = 100$ kg/mol, $T(R) = 395$ K, $R = 0.125$ μm) in a double-logarithmic

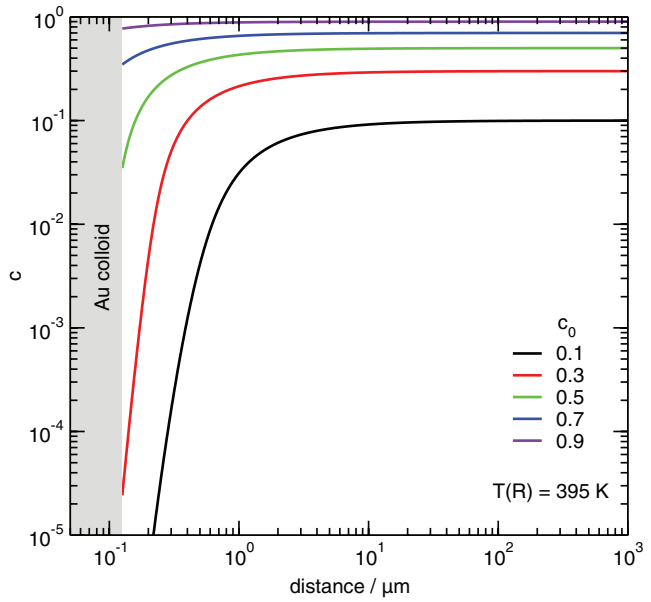

FIG. 6. Polymer concentration (mass fraction) as a function of the distance from the colloid for different initial concentrations c_0. Surface temperature $T(R) = 395$ K and molar mass $M = 100$ kg/mol.

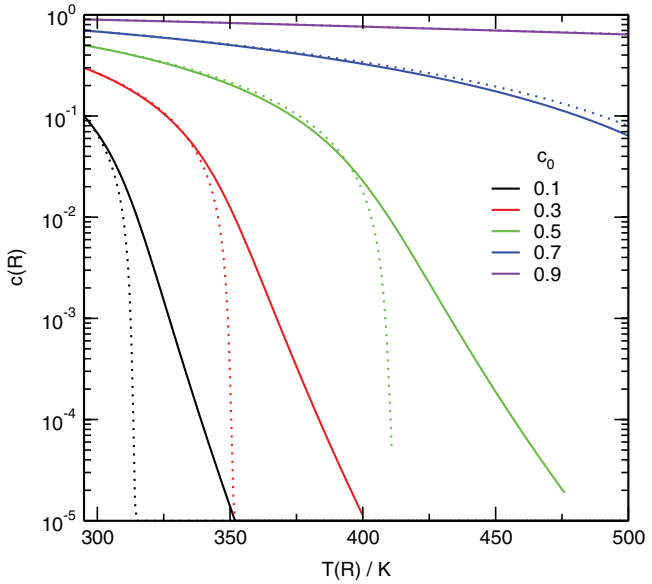

FIG. 7. Polymer concentration (mass fraction) at the surface of the colloid as a function of the surface temperature for different initial concentrations c_0. The polymer molar mass is 100 kg/*mol* and, for comparison, 10 000 kg/mol (dotted lines).

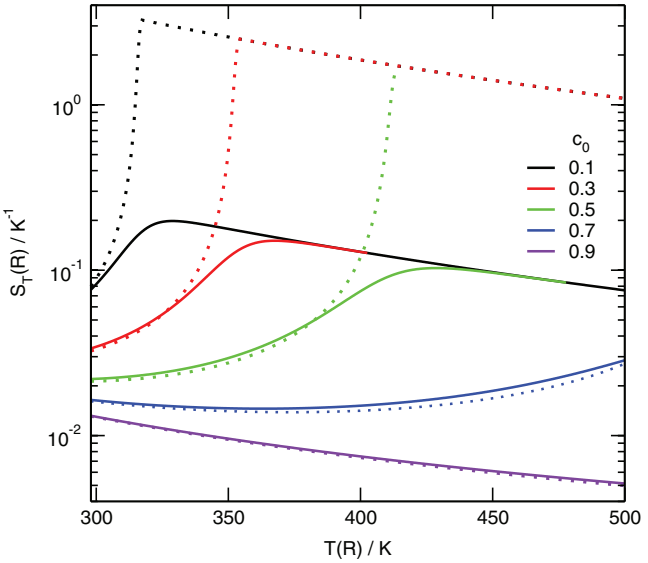

FIG. 8. Soret coefficient at the surface of the colloid as a function of the surface temperature for different initial polymer concentrations (mass fractions) c_0. The polymer molar mass is 100 kg/mol and, for comparison, 10 000 kg/mol (dotted lines).

representation for different initial concentrations c_0. For a very concentrated solution with $c_0 = 0.9$ only a shallow concentration dip is achieved, but already for $c_0 = 0.7$ the concentration change amounts to 50% .

The strong concentration and temperature dependence of the Soret coefficient leads to a pronounced nonlinear response of the concentration field with two competing mechanisms. A self-amplification of the effect is caused by the positive feedback loop due to the strong increase of S_T with decreasing polymer concentration. As shown in Fig. 2, this amplification can amount to more than two orders of magnitude in the case of very long polymer chains. The temperature dependence of $S_T \propto T^{-2.4}$, on the other hand, introduces a negative feedback loop that counteracts a further depletion of the polymer. Since the negative feedback loop is coupled to the – for a given laser intensity – invariant temperature profile and the positive feedback loop to the variable system-dependent concentration profile, quite complex scenarios can develop. The Soret coefficient can even pass through a maximum at a certain distance from the colloid.

In order to develop a better understanding of the various scenarios, it is instructive to investigate the stationary concentration $c(R)$ directly at the surface of the colloid. $c(R)$ is plotted for $M = 100$ kg/mol in Fig. 7 as a function of the colloid surface temperature for different initial concentrations. For $c_0 = 0.1$, a polymer depletion down to 1% of the initial value is achieved already at $T(R) \approx 325$ K and for $c_0 = 0.3$ around $T(R) \approx 360$ K.

The positive feedback loop is particularly effective in the case of long polymer chains. The strong increase of S_T with increasing M in the dilute limit leads to a complete depletion in the limit $M \to \infty$ as soon as sufficiently low concentrations are reached at the colloidal surface. To illustrate this, Fig. 7 contains, in addition to the results for $M = 100$ kg/mol, also some curves for $M = 10\,000$ kg/mol. Down to the semidilute regime of the shorter polymer there is hardly any difference between both molar masses. As soon as the dilute regime of the shorter polymer is reached, around $c \approx 0.01$, S_T of this polymer settles at its dilute limit and $c(R)$ decays with a long tail towards high surface temperatures $T(R)$. The concentration of the $M = 10\,000$ kg/mol-polymer continues its rapid drop to zero, fueled by a continuously increasing Soret coefficient as shown in Fig. 8. Once the dilute limit is reached, S_T passes through its maximum value and then decays again due to the increasing temperature. For very high polymer concentrations, the negative feedback prevails and no increase of $S_T(R)$ is observed over the entire temperature range ($c_0 = 0.9$ in Fig. 8).

The decisive influence of the molar mass becomes apparent from Fig. 9, which shows the polymer concentration at the surface for a fixed surface temperature of $T(R) = 395$ K as a function of the polymer molar mass. For the two lowest initial concentrations ($c_0 = 0.1$ and $c_0 = 0.3$), there is a complete depletion already for comparatively short chains ($M \approx 100$ kg/mol in the case of $c_0 = 0.3$), but already for $c_0 = 0.5$ it is impossible to remove the polymer completely from the colloid, no matter how high the molar mass. The transition occurs slightly above $c_0 = 0.4625$.

D. The viscosity profile

The temperature and composition change of the matrix around the colloid leads to a dramatic change of the viscosity η on a very short sub-micrometer to micrometer length scale. There are three different and not directly related mechanisms that are responsible for this effect and that all act in the same direction, towards a reduction of the viscous friction experienced by the colloid.

The first effect is the decrease of η with increasing temperature that is already observed at constant composition. In

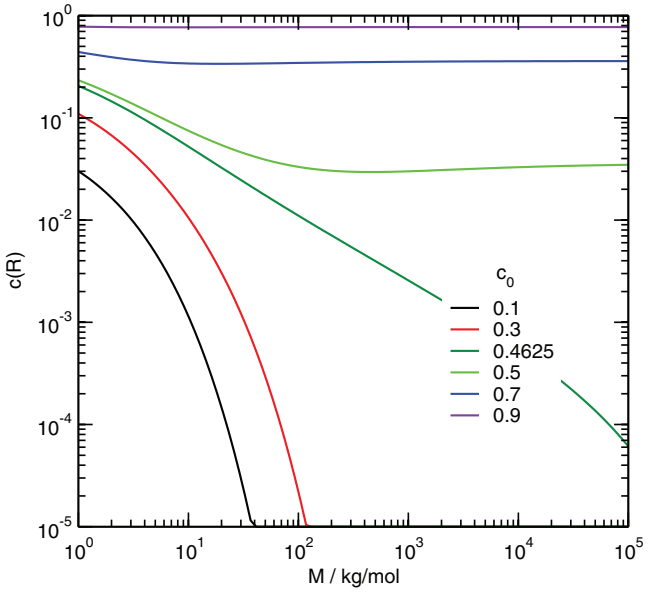

FIG. 9. Polymer concentration (mass fraction) at the surface of the colloid as a function of the molar mass for a fixed surface temperature of $T(R) = 395$ K.

its simplest form it is described by an Arrhenius-like thermal activation, but in a supercooled liquid not too far away from the glass transition temperature T_g a WLF-(Williams-Landel-Ferry)-equation[28] (see below) yields a more adequate description. This change of the viscosity is directly coupled to the temperature field and localized in the same way.

The second mechanism is related to the concentration of the polymer. The zero shear viscosity of polymers strongly depends on molar mass and concentration. Short chains below the entanglement molar mass $M_e \approx 10$ kg/mol show Rouse dynamics in the bulk. Hydrodynamic coupling, as described by the Rouse-Zimm model, becomes increasingly important[29] in dilute solutions. For molar masses above M_e, as employed in our experiments, the polymer dynamics is dominated by entanglements. They form topological constraints that restrict motion to a tube along the contour of the chain. De Gennes' reptation model provides the theoretical framework for this polymer contribution to the viscosity.[18,30] It predicts a strong molar mass dependence for polymer melts, $\eta \sim M^3$, which is even surpassed by the experimental value of 3.4 for the exponent.

In particular for long polymer chains, there is also a very strong concentration dependence of η, which starts at the low viscosity of the pure solvent and increases up to the high viscosity of the entangled melt. Above the entanglement volume fraction ϕ_e, the concentration dependence of the specific viscosity η_{sp} is given by[31,32]

$$\eta_{sp} = \frac{\eta - \eta_s}{\eta_s} \sim \left(\frac{\phi}{\phi^*}\right)^{3/(3\nu-1)} \sim M^3\phi^{3.92}. \tag{12}$$

Here, $\nu = 0.588 \approx 0.6$ is the Flory exponent for an athermal solvent and the molar mass dependence has been introduced via the overlap volume fraction

$$\phi^* \sim \phi_e \sim M^{1-3\nu} \sim M^{-0.8} \overset{M\to\infty}{\longrightarrow} 0. \tag{13}$$

Note that ϕ^* and ϕ_e can become very small for long polymer chains. Volume and mass fractions are identical for our purposes.

For dilute solutions ($\phi < \phi^*$), the viscosity can be obtained from the Mark-Houwink-Sakurada equation[31] for the intrinsic viscosity

$$[\eta] = \lim_{c\to 0} \frac{\eta_{sp}}{c} = K_H M^{\alpha} = K_H M^{3\nu-1}. \tag{14}$$

Above scaling laws capture essential predictions of the reptation model but they do not provide numerical prefactors and still underestimate the true viscosity increase with concentration and chain length. For a decent quantitative description, we resort to an empirical parameterization of the viscosity η_p of semidilute PS/toluene solutions provided by Kulicke and Kniewske [33] and similarly by Adam and Delsanti[32]

$$\eta_p = \eta_s(T)\,\tilde{\eta}_p(c, M), \tag{15}$$
$$\tilde{\eta}_p(c, M) = CKM^{\alpha} + C^2K^2M^{2\alpha}K_H + C^nK^nM^{n\alpha}B_n + 1$$

with

$$\eta_s = 0.558\,\text{mPa s},$$
$$K = 8.62 \times 10^{-3},$$
$$\alpha = 0.736,$$
$$K_H = 0.40,$$
$$n = 4.55,$$
$$B_n = 2.474 \times 10^{-3},$$

where C is the concentration in g/cm^3, whose numerical value can be taken as approximately identical to the weight fraction c for practical purposes. M is the molar mass in g/mol. Above relation has been determined for semidilute solutions of PS/toluene up to ~10% polymer concentration at a temperature of 25 °C. It is, however, believed to describe the entanglement effect on the viscosity, which is obscured by the increasing microscopic friction for the monomers at higher concentrations and not directly observable in the pure form. In particular, Eq. (15) reproduces the correct scaling exponents for the molar mass and concentration dependence for semidilute solutions and is compatible with the Mark-Houwink-Sakurada equation (14) in the dilute limit.

The third mechanism that reduces the viscosity is related to the distance from the glass transition temperature T_g, which determines the microscopic friction experienced by the solvent molecules and the polymer segments. PS/toluene is a binary glass former with a high T_g contrast of $T_g^s = 117$ K (Ref. 34) and $T_g^p \approx 373$ K (Refs. 19 and 35) for the solvent and the polymer, respectively. Consequently, not only a temperature but also a composition variation leads to a change of the distance to the glass transition temperature and strongly affects all dynamical processes.[9]

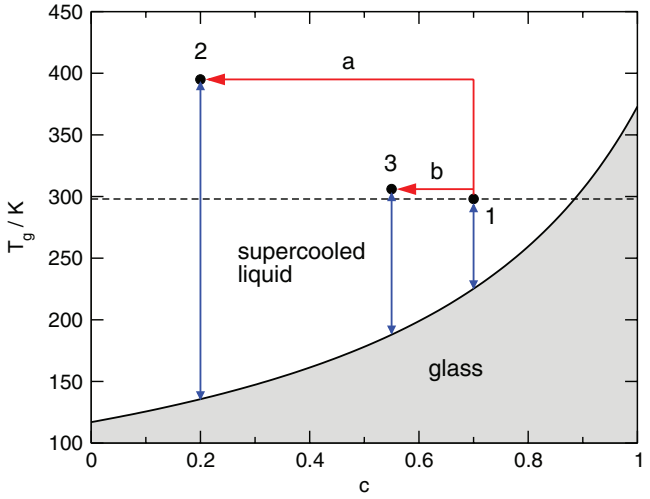

FIG. 10. Glass transition temperature T_g of a PS/toluene solution vs. polymer concentration (mass fraction) c as estimated from Eq. (16). (a) and (b) denote concentration and temperature changes at different positions of the sample.

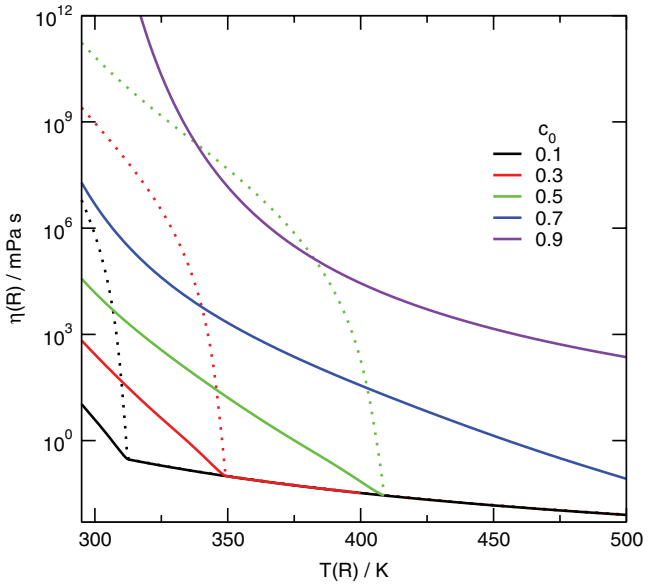

FIG. 11. Viscosity at the surface of the colloid as a function of the surface temperature for different initial polymer concentrations (mass fractions) c_0. See Fig. 7 for corresponding concentration changes and Fig. 8 for Soret coefficients. The polymer molar mass is 100 kg/mol and, for comparison, 10 000 kg/mol (dotted lines).

For an estimation of T_g of the solution of polymer concentration c we resort to the Fox-equation[36]

$$\frac{1}{T_g} = \frac{c}{T_g^p} + \frac{1-c}{T_g^s}. \tag{16}$$

Fig. 10 shows hypothetical but not unrealistic temperature and concentration excursions for two different distances from the colloid. Directly at the surface (scenario *a*) there is both a strong increase in temperature and a strong decrease in polymer concentration, either one increasing the distance to T_g. One micrometer away from the colloid there is only ∼10% of the temperature change left, but the concentration shift may still be significant due to the nonlinear nature of the concentration bleaching (scenario *b*). Also in this case a noticeable decrease in viscosity that is attributable to the increasing distance to the glass transition is expected.

To account for the effect of the supercooled liquid we use a WLF-(Williams-Landel-Ferry)-type shift factor[28]

$$\log a_T = -\frac{C_1^g (T - T_g(c))}{C_2^g + (T - T_g(c))} \tag{17}$$

with the universal values $C_1^g = 17.4$ and $C_2^g = 51.6\,\mathrm{K}$.[37] Although, strictly speaking, Eq. (17) only holds up to 50 … 100 K above T_g and does not reproduce the correct activation energies above these temperatures,[28] it can still be employed to capture the essential features.

Combining the effects of entanglements (Eq. (15)) and glass transition (Eq. (17)), we obtain the final expression for the temperature, concentration, and molar mass dependence of the viscosity

$$\log \eta(T, c, M) = \log \eta_s(T_0) + \log \tilde{\eta}_p(c, M) + \log a_T(T, c) - \log a_T(T_0, 0), \tag{18}$$

here, T_0 is an arbitrary reference temperature, which we have chosen as $T_0 = 298$ K for convenience.

Above Eq. (18) provides an expression for the macroscopic shear viscosity. It contains two very different contributions that act on different length scales. The slowing down of the supercooled liquid affects all motions on the scale of the solvent molecules and polymer segments. Their dynamics sets the pace for the release of the topological constraints of the polymer chains. These entanglements severely affect the macroscopic viscosity, but they do not contribute to the friction experienced by a small entity of the size of a solvent molecule. The length scale for which entanglements become important is set by the size of the entanglement strands. An upper limit can be estimated by the radius of gyration, which is significantly below the radius of our colloids. Hence, it is reasonable to estimate the friction by the macroscopic shear viscosity, but this may be a matter of discussion in the case of very small nanometer-sized colloids. The viscosity change near the colloid surface that corresponds to the scenarios in Figs. 7 and 8 is shown in Fig. 11. In particular for the high molar masses dramatic reductions of η can be achieved already by only moderate heating of the colloids by a few degrees.

Fig. 12 shows the *relative* change of the viscosity at the colloid surface ($T(R) = 395$ K) as a function of M for different initial concentrations c_0. Clearly, two different regimes can be distinguished. The almost horizontal (molar mass independent) regions are characteristic for the "glass effect," where the viscosity change is mainly due to change of the distance to T_g by both the temperature and concentration change. It becomes more pronounced with increasing polymer concentration due to the strong nonlinearity of the WLF equation. This mechanism also prevails for large M at high concentrations, where no quantitative concentration bleaching is possible.

The power law regions with a slope of –3.35 are characteristics for the entanglement effect on the equilibrium polymer viscosity. They are observed in situations where the polymer is completely depleted at the particle surface.

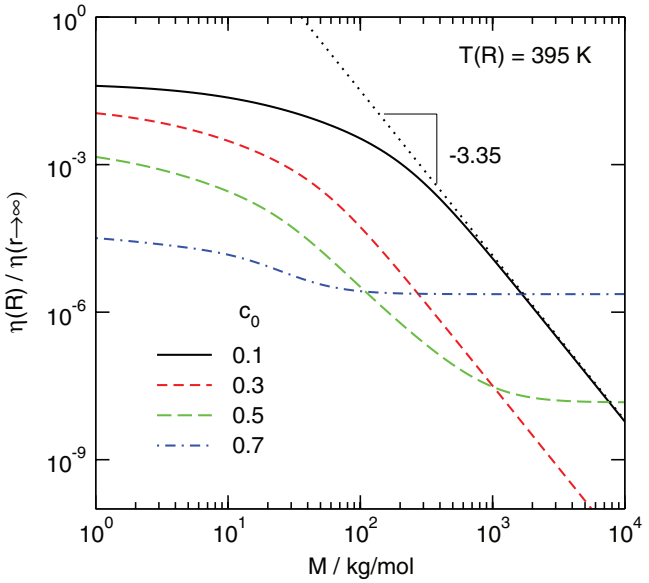

FIG. 12. Relative viscosity change at the surface of the colloid as a function of the polymer molar mass for different initial polymer concentrations (mass fractions) c_0 for a fixed surface temperature of $T(R) = 395$ K.

E. Time scales

So far we have only dealt with the stationary state, where we have found that the viscosity in the immediate vicinity of the colloidal particle can dramatically be reduced due to the depletion of the polymer. The plain temperature dependence of η additionally adds to the effect but is much less important. Although the focus of the present work is not on dynamics, it is instructive to shed some light on the time scales of the various processes, since these have direct consequences for the environment of a moving particle.

Every time the colloid is displaced, either by a random diffusive step or due to some external force acting on the particle, the original temperature and polymer concentration profiles no longer correspond to the new stationary state. During intermediate times, until the new stationary state has developed, the colloid "feels" the rim of the concentration bubble and an anisotropic viscosity profile. Recently, it has been shown that such a situation can lead to sub- or super-diffusive motion on intermediate time scales.[38]

Although there is no intrinsic length scale in the power law decay of $T(r)$, we can take a characteristic length of $l \approx 1\ \mu$m for the comparison of the various time scales. Almost 90% of the temperature change occurs within a sphere of this radius and also the major portion of the concentration bubble is confined within this sphere as long as excessive saturation of the concentration bleaching is avoided (Fig. 6).

Due to the high value of the thermal diffusivity ($D_{th} \approx 10^{-3}$ cm^2/s), the thermal relaxation time, which is the time needed to establish the temperature profile, is only $\tau_{th} \sim l^2/D_{th} = 10^{-5}$s.

The diffusion coefficient of the colloid can be estimated from the Stokes Einstein relation $D_c = kT(6\pi\eta R)^{-1}$. Depending on the polymer concentration, the viscosity varies dramatically, but in the case of quantitative polymer depletion around the center of the bubble, η can be approximated by the viscosity of the solvent. Neglecting the temperature variation, the diffusion coefficient is $D_c \approx 3 \times 10^{-8}$ cm^2/s and the characteristic colloid diffusion time $\tau_c \sim l^2/D_c = 0.3$ s.

The collective diffusion coefficient D_p of the polymer determines the time scale of the formation of the concentration bubble. It is practically identical to one of the colloids in the dilute limit ($M = 10\,000$ kg/mol). Above the overlap concentration, diffusion of the entangled polymer solution becomes faster and reaches a maximum value of $D_p \approx 2 \times 10^{-6}$ cm^2/s around $c \approx 0.3$. At even higher concentrations it slows down because of the reduced distance to the glass transition. Slightly above $c \approx 0.8$, D_p again becomes comparable to D_c.[9]

Due to the strong concentration dependence of D_p, the formation of the bubble cannot be characterized by a single time constant. What can be said without numerical in-depth analysis of the dynamics of the system is that diffusion of the colloid near the center and bubble reformation occur on comparable time scales and significant coupling between both motions can be expected. This may be even more severe in the case of additional external fields that impose a drift on the colloids.

III. SUMMARY AND CONCLUSIONS

We have investigated the transient cage formation around gold colloids embedded in polymer solutions, which can easily be heated by laser irradiation into their plasmon resonance absorption band. In systems with a positive Soret coefficient of the polymer, such as PS/toluene, the polymer is repelled from the immediate vicinity of the colloid and a localized solvent-rich bubble develops around the particle. Due to the complex concentration and temperature dependence of the Soret coefficient, there is a competition between attenuation and self-amplification. Depending on the polymer molar mass, the initial concentration, and the colloid surface temperature, the local polymer concentration can settle at a reduced yet finite value or can even drop to practically zero. Since the complete molar mass, concentration, and temperature dependence of $S_T(M, c, T)$ is known, the stationary state could be obtained from a numerical solution of the extended diffusion equation, incorporating both isothermal mass and non-isothermal thermal diffusion mechanisms.

Of particular interest for a future study of the associated dynamics are two scenarios where a concentration change is accompanied by dramatic changes of the local viscosity. The first one is observed at high polymer concentrations, where the solution approaches the glass transition. Due to the high T_g-contrast of toluene and PS both the temperature increase and the polymer depletion act in the same direction towards a lowering of the viscosity. Because of the relatively small value of S_T in concentrated polymer solutions and its decrease with increasing temperature, the effect is self-attenuated and polymer depletion is limited to some finite value, independent of the molar mass in the high polymer regime (Fig. 9).

The second scenario comprises dilute solutions of very long chains. There, the viscosity increases dramatically in the semidilute regime, which is already reached for very low concentrations below 1%. This is the regime of self-amplification, where dilution leads to a continuous increase of S_T, which in

turn fuels the polymer depletion. In these systems, the polymer can entirely be removed from the colloid with a rather moderate temperature increase as shown in Fig. 11.

Besides the visualization of the stationary solvent bubble, first qualitative experiments have shown the expected dramatic enhancement of the mobility of the colloid within its dynamically self-created environment. Future experiments will have to deal quantitatively with the dynamical aspects, such as enhanced and non-Fickian diffusion and the coupling between the particle motion and the retarded reformation of the bubble. Although most polymers in solution have a positive Soret coefficient, there are also systems with negative S_T,[39] where the polymer would be attracted to the colloid and slow down or even jam its motion.

ACKNOWLEDGMENTS

F.S. thanks S. Hartmann for help with the TDFRS measurements. This work has been supported by the Deutsche Forschungsgemeinschaft (Research Unit FOR608/TP6).

[1]M.-A. Neouze and U. Schubert, Monatsch. Chem. **139**, 183 (2008).
[2]D. Weitz and M. Oliveria, Phys. Rev. Lett. **52**, 1433 (1984).
[3]Y. Zhang, C. Gu, A. M. Schwartzberg, S. Chen, and J. Z. Zhang, Phys. Rev. B **73**, 165405 (2006).
[4]P. M. Hansen, V. K. Bhatia, N. Harrit, and L. Oddershede, Nano Lett. **5**, 1937 (2005).
[5]C. D. Jones and L. A. Lyon, J. Am. Chem. Soc. **125**, 460 (2003).
[6]D. Rings, R. Schachoff, M. Selmke, F. Cichos, and K. Kroy, Phys. Rev. Lett. **105**, 090604 (2010).
[7]S. R. de Groot and P. Mazur, *Non-Equilibrium Thermodynamics* (Dover, New York, 1984).
[8]J. K. Platten, M. M. Bou-Ali, P. Costesèque, J. F. Dutrieux, W. Köhler, C. Leppla, S. Wiegand, and G. Wittko, Philos. Mag. **83**, 1965 (2003).
[9]J. Rauch and W. Köhler, J. Chem. Phys. **119**, 11977 (2003).
[10]R. Piazza and A. Parola, J. Phys. Condens. Matter **20**, 153102 (2008).
[11]M. Giglio and A. Vendramini, Phys. Rev. Lett. **34**, 561 (1975).
[12]W. Enge and W. Köhler, Phys. Chem. Chem. Phys. **6**, 2373 (2004).
[13]R. Sigel, G. Fytas, N. Vainos, S. Pispas, and N. Hadjichristidis, Science **297**, 66 (2002).
[14]M. Anyfantakis, B. Loppinet, G. Fytas, and S. Pispas, Opt. Lett. **33**, 2839 (2008).
[15]W. Köhler, A. Krekhov, and W. Zimmermann, Adv. Polym. Sci. **227**, 145 (2010).
[16]A. Voit, A. Krekhov, and W. Köhler, Phys. Rev. E **76**, 011808 (2007).
[17]A. Voit, A. Krekhov, W. Enge, L. Kramer, and W. Köhler, Phys. Rev. Lett. **94**, 214501 (2005).
[18]M. Doi and S. F. Edwards, *The Theory of Polymer Dynamics* (Oxford University Press, New York, 1986).
[19]C. M. Roland and R. Casalini, J. Chem. Phys. **119**, 1838 (2003).
[20]H. S. Carslaw and J. C. Jaeger, *Conduction of Heat in Solids* (Oxford University Press, New York, 1973).
[21]M. A. van Dijk, A. L. Tchebotareva, M. Orrit, M. Lippitz, S. Berciaud, D. Lasne, L. Cognet, and B. Lounis, Phys. Chem. Chem. Phys. **8**, 3486 (2006).
[22]J. Rauch, Ph.D. dissertation, University of Bayreuth, 2005.
[23]J. Rauch and W. Köhler, Macromolecules **38**, 3571 (2005).
[24]D. Stadelmaier and W. Köhler, Macromolecules **41**, 6205 (2008).
[25]J. Rauch and W. Köhler, Phys. Rev. Lett. **88**, 185901 (2002).
[26]K. J. Zhang, M. E. Briggs, R. W. Gammon, J. V. Sengers, and J. F. Douglas, J. Chem. Phys. **111**, 2270 (1999).
[27]G. Wittko and W. Köhler, Philos. Mag. **83**, 1973 (2003).
[28]M. L. Williams, R. F. Landel, and J. D. Ferry, J. Am. Chem. Soc. **77**, 3701 (1955).
[29]H. C. Öttinger, Colloid Polym. Sci. **265**, 101 (1987).
[30]P. G. de Gennes, J. Chem. Phys. **55**, 572 (1971).
[31]M. Rubinstein and R. Colby, *Polymer Physics* (Oxford University Press, Oxford, 2005).
[32]M. Adam and M. Delsanti, J. Phys. (France) **44**, 1185 (1983).
[33]W.-M. Kulicke and R. Kniewske, Rheol. Acta **23**, 75 (1983).
[34]J. Wiedersich, N. V. Surovtsev, and E. Rössler, J. Chem. Phys. **113**, 1143 (2000).
[35]J. Rieger, J. Therm Anal. Calorim. **46**, 965 (1996).
[36]T. G. Fox, Bull. Am. Phys. Soc. **1**, 123 (1956).
[37]T. Masuko, M. Sato, and M. Karasawa, J. Appl. Polym. Sci. **22**, 1431 (1978).
[38]M. Burgis, V. Schaller, M. Glässl, B. Kaiser, W. Köhler, A. Krekhov, and W. Zimmermann, New J. Phys. **13**, 043031 (2011).
[39]B.-J. de Gans, R. Kita, B. Müller, and S. Wiegand, J. Chem. Phys. **118**, 8073 (2003).